Convolving Directed Graph Edges via Hodge Laplacian for Brain Network Analysis

Joonhyuk Park[1], Yechan Hwang[1], Minjeong Kim[2], Moo K. Chung[3], Guorong Wu[4], and Won Hwa Kim[1(✉)]

[1] Pohang University of Science and Technology, Pohang, South Korea
{pjh1023,yechan99,wonhwa}@postech.ac.kr
[2] University of North Carolina at Greensboro, Greensboro, USA
[3] University of Wisconsin - Madison, Madison, USA
[4] University of North Carolina at Chapel Hill, Chapel Hill, USA

Abstract. A brain network, viewed as a graph wiring different regions of interest (ROIs) in the brain, has been widely used to investigate brain dysfunction with various graph neural networks (GNNs). However, existing GNNs are built upon graph convolution that transforms measurements on the nodes, where ROI-wise features are not always guaranteed for brain networks. Therefore, the majority of existing graph analysis methods that rely on node features are inapplicable for network analysis unless a proxy such as node degree is provided. Moreover, the complex neurological interactions across different brain regions cannot be directly expressed in a simple node-to-node (i.e., 0-simplex) representation. In this paper, we propose a novel method, Hodge-Graph Neural Network (Hodge-GNN), that allows the GNN to directly derive desirable representations of graph edges and capture complex edge-wise topological features spatially via the Hodge Laplacian. Specifically, representing a graph as a simplicial complex holds a significant advantage over conventional methods that extract higher-order connectivity of a graph through hierarchical convolution in the spatial domain or graph transformation. The superiority of our method is validated in the Alzheimer's Disease Neuroimaging Initiative (ADNI) study, in comparison to benchmarking GNNs as well as state-of-the-art graph classification models.

Keywords: Hodge Laplacian · Brain Network · Alzheimer's Disease

1 Introduction

The wiring system within the human brain can be modeled as a complex graph, where the anatomical regions of interest (ROIs) are represented as nodes, and

J. Park and Y. Hwang—contributed equally to this paper.

Supplementary Information The online version contains supplementary material available at https://doi.org/10.1007/978-3-031-43904-9_76.

H. Greenspan et al. (Eds.): MICCAI 2023, LNCS 14224, pp. 789–799, 2023.
https://doi.org/10.1007/978-3-031-43904-9_76

the white matter connectomes define edges between them [9,18]. The graph-based representation explains actual connections between different nodes, and thus brain network analysis has a significant advantage over traditional spatial analysis to investigate interactions of different ROIs. As various neurodegenerative disorders such as Alzheimer's Disease (AD) are understood as a disconnection syndrome [2,9], studies on the structural connectivities in the brain are of significant interest from both machine learning and clinical perspectives.

Recently, variants of graph neural networks (GNNs) have been successful in brain network analysis with feature aggregation and message-passing mechanism on graph nodes [4,5,18]. Notice that, regardless of whether it is spatial or spectral, existing methods heavily rely on graph convolution that operates with the node signals (i.e., ROI measures). Here, the topology of graph plays an indirect role as the domain of the signal, merely selecting specific neighborhood for feature aggregation. The problem becomes even more severe when it comes to actual connectivity analysis *without* ROI-wise measurements. To utilize GNN methods, auxiliary node-wise measures such as node degree and clustering coefficients are required to perform prediction tasks on the brain networks, and the contribution of connectomic features as a biomarker is often not fully investigated. To perform convolution on edges directly, heuristics such as line graph [15] or defining orthogonal matrices from graph Laplacian [21] exists, but they have disadvantages when the graph is directed or has many components.

In order to analyze the connectivity of brain networks directly, we propose a novel graph learning framework that allows a neural network to utilize the topological features by representing the brain network as a simplicial complex. We utilize the Hodge 1-Laplacian, i.e., $\mathcal{L}_1$; in geometry, the 1-simplex denotes a line segment, and the Hodge Laplacian $\mathcal{L}_1$ includes connection between different line segments (i.e., edges) in a graph depending on their directions. Leveraging the Hodge Laplacian lets us obtain directed relationships between graph edges (i.e., a brain network) as an undirected graph (i.e., Hodge Laplacian), and the edge weights in the original graph become a signal on the nodes comprehended by the Hodge Laplacian. Spatial convolution with the $\mathcal{L}_1$ combines directed edge weights of the original graph based on the nodes that they are sharing. Together with a spatial graph convolution formulation, we construct our Hodge-Graph Neural Network (Hodge-GNN) which predicts labels of graphs purely based on the topology of the graphs without any node measures.

The **contributions** of our work are **1)** proposing a novel graph edge-learning framework on higher-order connectivity (i.e., connectivity between edges) of graphs with Hodge Laplacian, **2)** defining spatial edge convolution layer that operates on graph edges directly, and **3)** demonstrating superior performance on graph classification with brain connectivity from Alzheimer's Disease Neuroimaging Initiative (ADNI) with interpretability. Using Hodge-GNN, we depict brain connectivities that are highly associated with AD classification, which are corroborated by prior AD literature.

2 Related Work

Higher-order connectivity in Spatial domain. To capture the relation of higher-order graph structures, Morris et al. [24,25] proposed hierarchical k-GNNs, which are hierarchical GNN architectures based on the k-dimensional Weisfeiler-Lehman (WL) algorithm. By performing message passing directly between subgraph structures, k-GNNs enable the network to capture structural information that is not observable at the node-level. Despite their superiority over 1-GNN, k-GNNs require large memory and high computational cost due to their stacking of models, showing limitation in scalability and effectiveness on large graphs. The authors in [4] define range with diffusion instead of hop-distances and train on the range to obtain desirable node-embeddings.

Line Graphs. Line graph transformation interchanges the nodes and edges in the original graph respectively, allowing the node-wise graph convolution to be performed edge-wise, which makes the learning of edge-embeddings feasible [15]. However, line graphs lack the property of injectivity, which implies that different graphs can be transformed into a same line graph.

Edge Convolution. [30] performed *edge convolution* by creating edge-embeddings from neighboring pair of point clouds. However, the suggested method requires node features to generate the edge-embeddings without any graph prior, and thus it requires rich node features to construct strong embeddings.

Spectral Filtering of Graph Edges. Huang et al. [14] defined spectral filters for graph signals of nodes and edges using the k-th Hodge Laplacian (HL) operators, i.e., HL-node and HL-edge, and showed effectiveness of capturing the edge-wise relation in heterogeneous brain functional networks. The authors in [21] performed kernel filtering in the spectral domain with a specialized orthonormal graph transform.

3 Preliminaries: Simplicial Complex Representation

A simplicial complex is a collection of simplices with various dimensional representations, where simplices refer to the basic blocks to represent objects in topological space. In detail, each simplex of various dimension can be seen as nodes (0-simplex), edges (1-simplex), triangles (2-simplex), and other higher dimensional counterparts. A simplicial complex composed of only 0-simplices is called a 0-skeleton, likewise, p-skeleton is composed of 0 to p-simplices. A graph, therefore, is a 1-skeleton with 0- and 1-simplices (nodes and edges) [1,14,19].

In a simplicial complex, a p-chain is defined as a sum of p-simplicies, denoted as $c = \sum_i \alpha_i \sigma^i$, where σ^i are the p-simplices and the α_i are either 0 or 1 [8]. A chain complex is defined as the sequence of groups, each of which is made

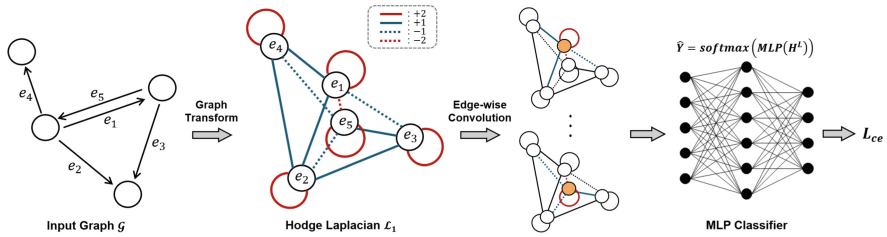

Fig. 1. The overall process of the proposed method: 1) deriving Hodge Laplacian $\mathcal{L}_1$ from input graph $\mathcal{G}$. 2) edge-wise graph convolution on e with $\mathcal{L}_1$. 3) Each edge (orange node) aggregates the information of neighboring edges in different weights given by $\mathcal{L}_1$. 4) MLP takes edge-convolved features as an input and is updated by the loss.

up of p-chains. To represent the relationship between chain groups, a boundary operator $\partial_p : C_p \rightarrow C_{p-1}$ is defined. Here, C_p denotes the p-th chain group, and the boundary operator ∂_p maps p-simplex to its boundaries ($(p-1)$-simplex). For an oriented p-simplex σ^p, the boundary operator can be defined as

$$\partial_p(\sigma^p) = \sum_{i=0}^{p} (-1)^i [v_0, v_1, \cdots, \hat{v_i}, \cdots, v_p], \tag{1}$$

where $[v_0, v_1, \cdots, \hat{v_i}, \cdots, v_p]$ is a $(p-1)$-simplex that is created by removing the vertex $\hat{v_i}$ from the p-simplex $\sigma^p = [v_0, v_1, \cdots, v_p]$ [1]. Also, the boundary operator ∂_p is represented using a boundary matrix $\mathcal{B}_p$ to facilitate efficient computation of the Hodge Laplacian. The p-th boundary matrix $\mathcal{B}_p$ can be defined as [23],

$$\mathcal{B}_p(i,j) = \begin{cases} 1, & \text{if } \sigma_i^{p-1} \subset \sigma_j^p \text{ and } \sigma_i^{p-1} \sim \sigma_j^p \\ -1, & \text{if } \sigma_i^{p-1} \subset \sigma_j^p \text{ and } \sigma_i^{p-1} \nsim \sigma_j^p \\ 0, & \text{if } \sigma_i^{p-1} \not\subset \sigma_j^p \end{cases} \tag{2}$$

where σ_i^p is the i-th p-simplex, and $\sim$ and $\nsim$ denote similar and dissimilar orientations respectively. The boundary matrix $\mathcal{B}_p$ relates the two adjacent simplices, i.e., p- and $(p-1)$-simplex, which will be used to define the Hodge Laplacian for higher-order graph representation in Sec. 4.1.

4 Proposed Method

The proposed method is composed of two components; graph transformation of adjacency matrix to Hodge Laplacian $\mathcal{L}_1$ with edge-wise features, and edge-wise graph convolution using the $\mathcal{L}_1$. With the traditional graph convolution formulation, the network can conduct transform of topological features directly instead of using them as indirect measures in previous GNNs.

4.1 Hodge Laplacian of Brain Network Data

Let $\mathcal{G} = (\mathcal{V}, \mathcal{E})$ be a directed weighted graph, where $\mathcal{V}$ is a set of nodes, and $\mathcal{E}$ is a set of directed edges consisting of ordered tuples, (u, v), s.t. $u, v \in \mathcal{V}$, which denotes an edge from u to v. $\mathcal{E}$ is indexed with $\{e_i\}_{i=1}^{E}$, $|\mathcal{E}| = E$ is the number of edges, and $|\mathcal{V}| = N$ is the number of nodes.

Hodge Laplacian $\mathcal{L}_p$, also known as the p-Laplacian is a generalization of graph Laplacian on higher simplices, i.e., nodes (0-simplices) to p-simplices. The Hodge Laplacian $\mathcal{L}_p$ is defined using the $\mathcal{B}_p(i, j)$ in Eq. (2) as:

$$\mathcal{L}_p = \mathcal{B}_p^T \mathcal{B}_p + \mathcal{B}_{p+1} \mathcal{B}_{p+1}^T. \tag{3}$$

From Eq. (3), the Hodge 0-Laplacian, $\mathcal{L}_0$, is equivalent to graph Laplacian, defined as $\mathcal{L}_0 = \mathcal{B}_1 \mathcal{B}_1^T$, where $\mathcal{B}_1 \in \mathbb{R}^{N \times E}$ is a boundary matrix for the 1-simplex, i.e., an incidence matrix relating nodes to edges.

To enable the graph representation to hold connectivity over edges, we construct Hodge Laplacian $\mathcal{L}_1$. As a 1-skeleton, i.e. topological graph, is composed of 0 and 1 simplex only (i.e., $\mathcal{B}_2 = 0$), the $\mathcal{L}_1 \in \mathbb{R}^{E \times E}$ is derived as:

$$\mathcal{L}_1 = \mathcal{B}_1^T \mathcal{B}_1. \tag{4}$$

Considering the vertices $u, v, t \in \mathcal{V}$, s.t. $u \neq v \neq t$, each element $\mathcal{L}_1(i, j)$ is defined as:

$$\mathcal{L}_1(i,j) = \begin{cases} 2 & e_i = e_j \\ -2 & e_i = (u,v), e_j = (v,u) \\ 1 & (e_i = (u,v), e_j = (u,t)) \text{ or } (e_i = (u,v), e_j = (t,v)) \\ -1 & (e_i = (u,v), e_j = (t,u)) \text{ or } (e_i = (u,v), e_j = (v,t)) \\ 0 & \text{otherwise} \end{cases}. \tag{5}$$

A directed weighted graph $\mathcal{G}$ can be represented as a binary adjacency matrix $A \in \mathbb{R}^{N \times N}$ and a weight matrix $\mathcal{W} \in \mathbb{R}^{N \times N}$ for A. Since $\mathcal{W}$ holds features for each edge, we can extract the non-zero components of $\mathcal{W}$, which serves as a signal $\mathcal{W}_{\mathcal{E}} \in \mathbb{R}^{E}$ on $\mathcal{L}_1$.

4.2 Convolving Graph Edges via Hodge Laplacian $\mathcal{L}_1$

GCN [31] performs aggregation of the neighboring node features as:

$$H^{(l+1)} = \sigma(AH^{(l)}W^{(l)}), \qquad l = 0, \cdots, L, \tag{6}$$

where $A \in \mathbb{R}^{N \times N}$ is an adjacency matrix, and $W^{(l)}$ is a parameter matrix of the l-th layer. $H^{(l)} \in \mathbb{R}^{N \times K}$ is the output of the l-th convolution layer with K features, where $H^{(0)}$ is the input of node feature vectors, and $\sigma(\cdot)$ is a non-linear activation function. From a spatial perspective, the graph convolution relates the neighboring node features to generate the node embedding utilizing the adjacency matrix as a relational matrix that provides the direct neighboring information.

From a weighted adjacency matrix $A \in \mathbb{R}^{N \times N}$, we can extract Hodge Laplacian $\mathcal{L}_1 \in \mathbb{R}^{E \times E}$ and $W_{\mathcal{E}}$ which is a vector of edge weights considered as measurements on the nodes of $\mathcal{L}_1$. With $\mathcal{L}_1$, we construct a Hodge graph neural network (Hodge-GNN) whose l-th layer is defined as:

$$H^{(l+1)} = \sigma(\mathcal{L}_1 H^{(l)} W^{(l)}), \qquad l = 0, \cdots, L, \tag{7}$$

where $W^{(l)}$ is a learnable weight parameter and $H^{(l)} \in \mathbb{R}^{E \times K}$ is the output from the l-th convolution layer, with $H^{(0)} = \mathcal{W}_{\mathcal{E}}$. The key component here is $\mathcal{L}_1 H^{(l)}$, described as Edge-wise Convolution in Fig. 1.

When it comes to graph analysis, most of existing GNN methods assume that features on the nodes exist for node-wise analysis. However, when the measurements on the nodes do not exist, and the analysis must be performed solely with the graph topology and edge information, other GNN methods must define an auxiliary node-wise measures such as node degree and clustering coefficients. Unlike the previous approaches, our framework enables the information from adjacent edges to be given different weights, either positive or negative, depending on the topology of the graph, and the edge-wise convolution can now relate the edge features and generate edge embeddings, allowing the network to utilize the hidden topological features that were not seen in the original input graph form.

Finally, the class prediction $\hat{Y}^c$ for each class c is obtained by flattening the $H^{(L)} \in \mathbb{R}^{E \times K}$ and passing it through multi-layer perceptron (MLP), and applying a softmax yields

$$\hat{Y}^c = \frac{\mathrm{MLP}(H^{(L)})^c}{\sum_{c' \in C} \mathrm{MLP}(H^{(L)})^{c'}}. \tag{8}$$

The objective function defined by cross-entropy over all T samples is:

$$L_{ce} = -\sum_{t=1}^{T} \sum_{c \in C} Y_t^c log \hat{Y}_t^c, \tag{9}$$

where $Y_t^c = 1$ if the class of t-th graph is c, otherwise $Y_t^c = 0$.

4.3 Interpretability of the Connectomes in Brain Dysfunction

To provide interpretability to the framework, we define gradient-based class activation map on the graph edges using the formulation in [27,33]. Specifically, when a graph (i.e., $\mathcal{L}_1$ and $\mathcal{W}_{\mathcal{E}}$) is inputted to the network, by tracking the backpropagating gradients of the score for a specific class c (i.e., $\hat{Y}^c$) with regard to each feature vectors $H^k \in \mathbb{R}^{E \times 1}$ of the final convolution layer of GNN (i.e., $H^{(L)}$) [27], the importance of each activation α_k^c and the heatmap $\mathcal{H}$ of the specific class c can be computed as:

$$\mathcal{H}^c = ReLU\left(\frac{1}{K}\sum_k \alpha_k^c H^k\right), \quad \alpha_k^c = \frac{1}{Z}\sum_i \sum_j \left(\frac{\partial \hat{Y}^c}{\partial H_{ij}^k}\right). \tag{10}$$

Performing the edge-wise convolution from Hodge Laplacian $\mathcal{L}_1$, this heatmap $\mathcal{H}^c$ holds the contribution of each connectome to the classification of developmental stages in brain dysfunction (i.e., Alzheimer's Disease).

5 Experiments

5.1 Dataset and Experimental Settings

Dataset. Our dataset contains structural brain connectivity data derived from Diffusion Tensor Images (DTI) in Alzheimer's Disease Neuroimaging Initiative (ADNI) with tractography. Each sample is given as a directed weighted graph whose weights denote the *number of white matter fiber tracts* connecting two different ROIs and its corresponding diagnostic label. The ROIs and their connectomes were defined by the Destrieux atlas [7] with 148 cortical and 12 sub-cortical ROIs. As tractography involves probabilistic calculation, the connectivity matrix becomes non-symmetric with varying weights on the same connectivity matrices. The dataset is composed of n=1824 subjects within Control (CN, n=844), Early Mild Cognitive Impairment (EMCI, n=490), Late Mild Cognitive Impairment (LMCI, n=250), and AD (n=240) groups.

Table 1. Quantitative Comparison of Hodge-GNN with Baselines.

	Methods	Accuracy	Precision	Recall	F1-score
Conventional	SVM	58.31 ± 1.40	70.67 ± 3.44	44.49 ± 1.57	46.94 ± 2.36
	SLP	71.42 ± 3.42	68.91 ± 4.46	70.27 ± 3.39	69.16 ± 3.99
	MLP	72.41 ± 1.14	73.66 ± 1.29	67.47 ± 2.59	69.45 ± 1.22
	GCN ($\mathcal{G}$) [31]	70.16 ± 1.82	67.67 ± 2.46	66.82 ± 1.30	67.00 ± 1.88
	GCN ($\mathcal{G}_L$)	80.85 ± 3.10	81.21 ± 3.34	77.55 ± 2.93	79.09 ± 3.10
Spatial domain	1-2-GNN [25]	73.58 ± 1.12	71.44 ± 0.87	71.31 ± 1.41	71.15 ± 0.43
	1-2-3-GNN [25]	73.81 ± 1.91	72.39 ± 1.82	71.04 ± 2.64	71.25 ± 1.51
Spectral domain	MENET [21]	80.47 ± 1.82	79.30 ± 0.69	77.09 ± 1.59	77.92 ± 1.12
Edge Convolution	DGCNN [30]	72.61 ± 2.01	69.69 ± 2.29	69.11 ± 1.51	69.11 ± 1.90
Ours	Hodge-GNN	**83.60±1.93**	**84.75±2.19**	**80.10±1.87**	**82.03±1.93**

Edge Preprocessing. Unlike the widely used $A \in \mathbb{R}^{N \times N}$ or $\mathcal{L}_0 \in \mathbb{R}^{N \times N}$, the adoption of $\mathcal{L}_1 \in \mathbb{R}^{E \times E}$ incurs an exponential rise in both memory and computational costs. Also, the E across different samples varies from 2138 to 11802 (6766 in average). To handle such problems, we used the intersection of edges across entire samples. This preprocessing step yields the number of edges to be $E = 530$, common across all subjects.

Baselines. Our method is validated on various approaches, including conventional classification methods, neural networks, and graph methods of both spatial and spectral domain. In detail, we used support vector machine (SVM), single layer perceptron (SLP), multi-layer perceptron (MLP), and GCN [31] with original graph $\mathcal{G}$ and line graph $\mathcal{G}_L$ as the conventional classification method, as well as the hierarchical k-GNNs (1-2-GNN, 1-2-3-GNN) [25] and MENET [21] for spatial and spectral baselines respectively. Also, DGCNN [30] which extracts edge-embeddings with edge convolution from node features is compared as well.

Evaluation. 4-way classification is performed on the AD-specific groups. All models are evaluated using 5-fold cross validation (CV) for unbiased results. On the 4-way classification task for AD-specific groups, average accuracy, Macro-precision, Macro-recall, and Macro-F1-score (Table 1) are compared. Qualitative results of our experiment reveal the important connectivities in classifying AD stages (Fig. 2) from the trained model.

5.2 Experimental Results

Our Hodge-GNN is evaluated based on the 4-way classification of CN, EMCI, LMCI, and AD. The quantitative comparisons are shown in Tab. 1. As k-GNN, MEMET, and GCN with $\mathcal{G}_L$ capture higher-order connectivity information, they performed better than the conventional GCN with $\mathcal{G}$. However, Hodge-GNN was more effective in the AD classification, achieving the highest performance in all measures by ∼3%p over the second best method.

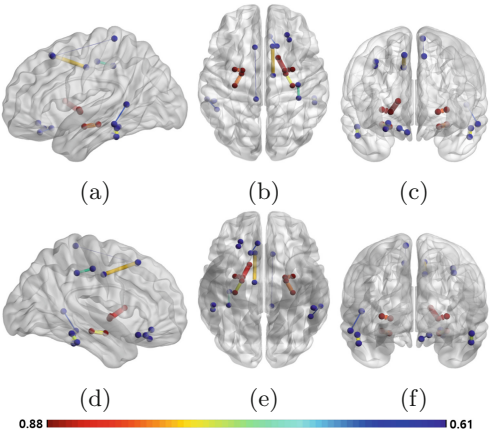

$\mathcal{H}$	ROI	ROI
0.883	Right-Pallidum	Right-Putamen
0.865	Left-Pallidum	Left-Putamen
0.833	Right-S_central	Right-S_postcentral
0.823	Left-G_subcallosal	Right-G_subcallosal
0.798	Left-S_temporal_inf	Left-G_temporal_inf
0.778	Right-Amygdala	Right-Hippocampus
0.776	Left-Amygdala	Left-Hippocampus
0.769	Right-S_orbital_med-olfact	Right-G_rectus
0.728	Right-Pallidum	Right-Thalamus-Proper
0.666	Right-S_temporal_inf	Right-G_temporal_inf
0.657	Left-G_and_S_paracentral	Left-G_front_sup
0.657	Right-G_and_S_cingul-Mid-Post	Right-G_front_sup
0.615	Left-S_temporal_sup	Left-G_temporal_middle

Fig. 2. Significant edges depicted from the AD analysis; (a),(d) outer view of left/right hemisphere, (b),(e) top/bottom, (c),(f) front/rear view. Blue node: cortical, Red node: subcortical region, Edge color/thickness denote class activation $\mathcal{H}$ from Eq. (10 (Color figure online)).

5.3 Interpretation of AD via Trained Hodge-GNN

Using the computed importance from Eq. (10), significant edges for classifying the stages of Alzheimer's Disease are depicted (Fig. 2). The significant edges are selected by taking intersection of the top-k edges for each class label. The top-k edges are the distinct edges obtained from the top-10 edges across the 5-fold cross validation. Thus, the selected edges represent common edges that shows high importance for classifying the brain dysfunction. During the progress of AD, ROIs of the brain show not only the shrinkage of volume but also weakening of connectivity [2,6]. As in Fig. 2, our classifier picked up connectome of ROIs in

the subcortical regions (i.e., amygdala, hippocampus, pallidum, putamen, and thalamus) [3,10,26], temporal lobe (i.e., inferior, middle, and superior temporal cortex) [3,10,11], frontal lobe (i.e., superior frontal gyrus) [10,16], and other important regions that are highly related to AD [12,20].

In addition, the depicted edges showed several symmetry found in both left and right hemispheres, such as pallidum-putamen and amygdala-hippocampus connectomes, both of which play a crucial role in the development of AD [13,29,32]. Interestingly, right pallidum was shared on two detected connectivities (i.e., with right-putamen and right-thalamus-proper), which highlights the importance of pallidum connectomes [17]. Also, out of the 17 ROIs consisting the detected connectivities, 5 ROIs (pallidum, amygdala, putamen, hippocampus, and thalamus) were from subcortical regions, denoting that they are critical for our AD-stage classification and subcortical areas are highly implicated in AD as in prior works [22,28].

6 Conclusion

We proposed a novel framework for extracting edge-to-edge relations in graph spatial domain using Hodge 1-Laplacian, i.e., Hodge-GNN. The Hodge-GNN performs graph convolution on edges via shared nodes among edges and allows a downstream predictor to accurately classify different stages of AD. The validation experiment showed superiority of performance in prediction together with interpretable outcomes depicting specific connectomes and ROIs for effective AD analysis.

Acknowledgement. This research was supported by NRF-2022R1A2C2092336 (50%), IITP-2022-0-00290 (20%), IITP-2019-0-01906 (AI Graduate Program at POSTECH, 10%) funded by MSIT, HU22C0171 (10%) and HU22C0168 (10%) funded by MOHW in South Korea, and NIH R03AG070701 from the US, and Foundation of Hope.

References

1. Anand, D.V., Chung, M.K.: Hodge-laplacian of brain networks and its application to modeling cycles. arXiv preprint arXiv:2110.14599 (2021)
2. Catani, M., Ffytche, D.H.: The rises and falls of disconnection syndromes. Brain **128**(10), 2224–2239 (2005)
3. Cheyuo, C., et al.: Connectomic neuromodulation for Alzheimer's disease: a systematic review and meta-analysis of invasive and non-invasive techniques. Transl. Psychiatry **12**(1), 490 (2022)
4. Choi, I., Wu, G., Kim, W.H.: How much to aggregate: learning adaptive node-wise scales on graphs for brain networks. In: Wang, L., Dou, Q., Fletcher, P.T., Speidel, S., Li, S. (eds.) Medical Image Computing and Computer Assisted Intervention – MICCAI 2022: 25th International Conference, Singapore, September 18–22, 2022, Proceedings, Part I, pp. 376–385. Springer, Cham (2022). https://doi.org/10.1007/978-3-031-16431-6_36

5. Cui, H., et al.: BrainGB: a benchmark for brain network analysis with graph neural networks. IEEE Trans. Med. Imaging **42**(2), 493–506 (2023)
6. Delbeuck, X., Van der Linden, M., Collette, F.: Alzheimer'disease as a disconnection syndrome? Neuropsychol. Rev. **13**, 79–92 (2003)
7. Destrieux, C., et al.: Automatic parcellation of human cortical gyri and sulci using standard anatomical nomenclature. Neuroimage **53**(1), 1–15 (2010)
8. Edelsbrunner, H., Harer, J.L.: Computational topology: an introduction. American Mathematical Society (2022)
9. Farahani, F.V., et al.: Application of graph theory for identifying connectivity patterns in human brain networks: a systematic review. Front. Neurosci. **13**, 585 (2019)
10. Filippi, M., et al.: Changes in functional and structural brain connectome along the Alzheimer's disease continuum. Mol. Psychiatry **25**(1), 230–239 (2020)
11. Galton, C.J., Patterson, K., et al.: Differing patterns of temporal atrophy in Alzheimer's disease and semantic dementia **57**(2), 216–225 (2001)
12. Gan, C., O'Sullivan, M., Metzler-Baddeley, C., et al.: Association of imaging abnormalities of the subcallosal septal area with Alzheimer's disease and mild cognitive impairment. Clin. Radiol. **72**(11), 915–922 (2017)
13. Guo, Z., et al.: Disrupted topological organization of functional brain networks in Alzheimer's disease patients with depressive symptoms. BMC Psychiatry **22**(1), 1–10 (2022)
14. Huang, J., Chung, M.K., Qiu, A.: Heterogeneous Graph Convolutional Neural Network via Hodge-Laplacian for Brain Functional Data. In: Frangi, A., de Bruijne, M., Wassermann, D., Navab, N. (eds.) Information Processing in Medical Imaging: 28th International Conference, IPMI 2023, San Carlos de Bariloche, Argentina, June 18–23, 2023, Proceedings, pp. 278–290. Springer, Cham (2023). https://doi.org/10.1007/978-3-031-34048-2_22
15. Jiang, X., Ji, P., Li, S.: CensNet: convolution with edge-node switching in graph neural networks. In: IJCAI, pp. 2656–2662 (2019)
16. Johnson, J.K., et al.: Clinical and pathological evidence for a frontal variant of Alzheimer disease. Arch. Neurol. **56**(10), 1233–1239 (10 1999)
17. Lehéricy, S., Hirsch, E.C., Hersh, L.B., et al.: Cholinergic neuronal loss in the globus pallidus of Alzheimer disease patients. Neurosci. Lett. **123**(2), 152–155 (1991)
18. Li, X., et al.: BrainGNN: interpretable brain graph neural network for fMRI analysis. Med. Image Anal. **74**, 102233 (2021)
19. Lim, L.H.: Hodge laplacians on graphs. arXiv preprint arXiv:1507.05379 (2015)
20. Lu, J., et al.: Functional connectivity between the resting-state olfactory network and the hippocampus in Alzheimer's disease. Brain Sci. **9**(12), 338 (2019)
21. Ma, X., Wu, G., Hwang, S.J., Kim, W.H.: Learning multi-resolution graph edge embedding for discovering brain network dysfunction in neurological disorders. In: Feragen, A., Sommer, S., Schnabel, J., Nielsen, M. (eds.) Information Processing in Medical Imaging: 27th International Conference, IPMI 2021, Virtual Event, June 28–June 30, 2021, Proceedings, pp. 253–266. Springer, Cham (2021). https://doi.org/10.1007/978-3-030-78191-0_20
22. McDuff, T., Sumi, S.: Subcortical degeneration in Alzheimer's disease. Neurology **35**(1), 123–123 (1985)
23. Meng, Z., Xia, K.: Persistent spectral-based machine learning (PerSpect ML) for protein-ligand binding affinity prediction. Sci. Adv. **7**(19), eabc5329 (2021)
24. Morris, C., Lipman, Y., Maron, H., et al.: Weisfeiler and leman go machine learning: the story so far. arXiv preprint arXiv:2112.09992 (2021)

25. Morris, C., Ritzert, M., Fey, M., et al.: Weisfeiler and leman go neural: Higher-order graph neural networks. In: AAAI, vol.33, pp.4602–4609 (2019)
26. Persson, K., Bohbot, V., Bogdanovic, N., et al.: Finding of increased caudate nucleus in patients with Alzheimer's disease. Acta Neurologica Scandinavica **137**(2), 224–232 (2018)
27. Selvaraju, R.R., Das, A., Vedantam, R., Cogswell, M., Parikh, D., Batra, D.: Grad-cam: Why did you say that? visual explanations from deep networks via gradient-based localization. CoRR abs/1610.02391 (2016)
28. Tentolouris-Piperas, V., Ryan, N.S., Thomas, D.L., Kinnunen, K.M.: Brain imaging evidence of early involvement of subcortical regions in familial and sporadic Alzheimer's disease. Brain Res. **1655**, 23–32 (2017)
29. Vogt, L.K., Hyman, B., Van Hoesen, G., Damasio, A.: Pathological alterations in the amygdala in Alzheimer's disease. Neuroscience **37**(2), 377–385 (1990)
30. Wang, Y., Sun, Y., Liu, Z., Sarma, S.E., Bronstein, M.M., Solomon, J.M.: Dynamic graph CNN for learning on point clouds. ACM Trans. Graph. **38**(5), 1–12 (2019)
31. Welling, M., Kipf, T.N.: Semi-supervised classification with graph convolutional networks. In: ICLR (2016)
32. West, M., Coleman, P., Flood, D., Troncoso, J.: Differences in the pattern of hippocampal neuronal loss in normal ageing and Alzheimer's disease. The Lancet **344**(8925), 769–772 (1994), originally published as Volume 2, Issue 8925
33. Zhou, B., Khosla, A., Lapedriza, A., et al.: Learning deep features for discriminative localization. In: CVPR. pp. 2921–2929 (2016)